https://doi.org/10.5194/egusphere-2025-3374
Preprint. Discussion started: 8 September 2025

Constrained attribution of changes in winds over the Southern Ocean from 1950 to 2100

Tereza Jarníková[1], Colin Jones[2], Steven Rumbold[3], Corinne Le Quéré[1]

[1] School of Environmental Sciences, University of East Anglia, UK
[2] National Centre for Atmospheric Science, University of Leeds, UK.
[3] National Centre for Atmospheric Science, University of Reading, UK

Correspondence to: Tereza Jarníková (T.Jarnikova@uea.ac.uk)

Abstract. Strong near-surface westerly winds drive the Southern Ocean circulation and play a key role in setting regional and global climate. In the latter half of the 20th century, depletion of stratospheric ozone over Antarctica has caused these winds to accelerate and move polewards, particularly in austral summer. However, the future evolution of these winds remains uncertain. We use reanalysis data and the UK Earth System Model (UKESM1), with full atmosphere interactive chemistry, to assess the drivers of the winds over the recent past and coming century. We first characterize the wind mean state, distribution, and trends over 1980-2020 in the most commonly used atmospheric reanalyses (ERA5, JRA3Q, MERRA2, and R1) to gain insights into observed wind behaviour in the past. We show that while the representation of the mean wind is similar among reanalyses, MERRA2 and R1 show stronger wind acceleration trends that persists year-round, while JRA3Q and ERA5 show weaker acceleration, primarily in austral summer. Using an observational Southern Annular Mode (SAM) index, we show that the weaker, summer-focused trends of JRA3Q and ERA5 are likely more accurate. UKESM1 represents historical trends in winds accurately compared to ERA5. Targeted model simulations show that ozone depletion is overwhelmingly responsible for the wind acceleration observed in 1980-2020, which occurs primarily in austral summer. The effect of ozone depletion on winds peaks in 1980-2000, when it is roughly double that for the entire 40-year period. Ozone recovery is then associated with a slowdown of winds from 2000 to 2050. Beyond 2050, the ozone effect becomes minimal and winds accelerate primarily due to greenhouse gas induced warming, with this trend more evenly distributed across seasons.

1 Introduction

Strong near-surface westerly winds are a dominant feature of the midlatitude atmospheric circulation over the Southern Ocean, driving the Antarctic Circumpolar Current (ACC), the largest ocean current on Earth. The ACC is an important control on the Atlantic Meridional Overturning Circulation (AMOC; J. Marshall & Speer, 2012) and plays a fundamental role in controlling Southern Ocean heat (Huguenin et al., 2022) and carbon uptake (Le Quéré et al., 2007).

Over the last four decades, substantial changes in the Southern Hemisphere wind regime have been seen in both reanalyses and observations. Chiefly, the wind jet (i.e., the location of the strongest westerly winds) has intensified and moved poleward (Swart & Fyfe, 2012), with substantial longitudinal variation (Goyal et al., 2021; Waugh et al., 2020). These changes are manifested in significant trends in the Southern Annular Mode (SAM; Fogt & Marshall, 2020).

https://doi.org/10.5194/egusphere-2025-3374
Preprint. Discussion started: 8 September 2025

The observed changes in southern hemisphere winds over the latter half of the 20th century have been linked to the depletion of stratospheric ozone, particularly the Antarctic ozone hole (Thompson & Solomon, 2002). The absorption of incoming solar UV radiation by ozone warms the stratosphere, so ozone depletion leads to a relative stratospheric cooling. This cooling strengthens the north-south temperature gradient, which in turn enhances the vertical wind shear and accelerates the polar vortex, especially in austral spring and summer (for an overview, see, e.g. Previdi & Polvani, 2014; Thompson et al., 2011). This acceleration results in an overall strengthening and poleward shift of Southern Ocean winds throughout the troposphere, particularly in austral summer (DJF), with an accompanying shift towards a more positive index of the SAM, the principal mode of atmospheric variability in the region (G. J. Marshall, 2003; Swart & Fyfe, 2012; Thompson et al., 2011).

This ozone-driven latitudinal shift and intensification is expected to reverse as Southern hemisphere ozone levels are projected to recover over the coming half century (Polvani et al., 2011; Solomon et al., 2017). Simultaneously, this slowdown is expected to be counteracted by a trend towards stronger and more southerly winds due to greenhouse gas-driven warming, year round (Arblaster et al., 2011; McLandress et al., 2011; Zambri et al., 2021). The future evolution of the overall wind patterns thus depends on which forcing dominates.

These changes in the Southern Hemisphere wind regime are likely to have multiple downstream effects on both the regional and global climate, and have thus attracted substantial research. However, differences in the representation of wind trends exist between reanalysis products, which may translate to differences in ocean responses when global ocean models are forced by different reanalyses (Friedlingstein et al., 2023; Tsujino et al., 2020) or have implications for energy production, as wind energy infrastructure depends on accurate estimates of regional wind state (Gualtieri, 2022). Furthermore, most studies to date have focused on the mean trend in the wind jet and omitted variability and extreme winds, which are disproportionately important for a number of ocean and climate processes, for example in rapid sea-ice loss (Jena et al., 2022), ice shelf calving events (Francis et al., 2020), and air-sea CO2 exchange (Gu et al., 2021).

In this paper, we examine recent changes in the Southern Ocean winds and quantify the relative contributions of stratospheric ozone depletion and rising greenhouse gas (GHG) concentrations in driving these changes. We first intercompare a suite of the most commonly used reanalysis products over the period 1980-2020, assessing the wind climatology and wind speed frequency distribution, as well as time trends in the mean wind speed, in extreme wind speeds, the position and variability of the wind jet, and the SAM index. We next evaluate the representation of the winds from the UK Earth System Model (UKESM1) against the reanalyses. Here we have two main applications in mind. First, we want to understand how suitable UKESM1 is for studying the wider climate effects of changes in the wind distribution – for example their role in modifying the uptake of carbon dioxide by the Southern Ocean (Jarníková et al., 2025). Second, we want to

https://doi.org/10.5194/egusphere-2025-3374
Preprint. Discussion started: 8 September 2025

understand to what extent this model can be used to attribute the relative contribution of ozone and greenhouse gases to changes in the wind distribution.

Finally, we attribute the relative drivers of historical changes in Southern Ocean winds and project their future evolution through to the end of the twenty first century. To do this, we perform a set of experiments with UKESM1 covering the period 1950-2100, modifying the emissions of Ozone Depleting Substances (ODS) to generate two stratospheric ozone scenarios (one with essentially no ozone loss and a second with historically accurate ozone evolution, i.e. Antarctic ozone depletion, followed by a subsequent recovery). These two ozone scenarios are each combined with two CMIP6 SSP scenarios that represent a high and low GHG emission scenario.

2 Methods

2.1 Selection of reanalyses and previous evaluation

Meteorological reanalyses provide a gridded estimate of the complete atmospheric state by assimilating satellite and in-situ observations within a numerical weather prediction model. A large number of global atmospheric reanalysis products are available (see https://reanalyses.org/ for an overview). Reanalyses are commonly used in climate monitoring and policy applications, as well as in fundamental research more broadly. For example, global and regional carbon cycle models are often forced by reanalysis products (Friedlingstein et al., 2023), so any differences between reanalyses may influence such studies.

We use a subset of the latest generation of products that are commonly used in earth system research: ERA5, JRA3Q, MERRA2, and R1 (NCEP-NCAR); The main characteristics of these reanalyses are given in Table 1. We initially also analyzed NCEP-DOE2, an update of R1, but ultimately excluded it because of anomalously large wind speed biases relative to the other four products. Spuriously high winds in NCEP-DOE2 have been noted previously. For example, Lucio-Eceiza et al. (2019) found that NCEP-DOE2 has worse performance than its predecessor R1 in estimating surface wind speeds in the North Atlantic, while Dong et al. (2020) found it had markedly worst performance in estimating Antarctic Ice Sheet winds compared to five other contemporary products.

Here we briefly survey some existing in-situ assessments of our chosen reanalyses and their predecessors, focusing on the Antarctic and Southern Ocean. Though a number of past studies have evaluated reanalysis winds in the Southern Ocean, the extent of past evaluation in the near-Antarctic region remains relatively limited because of the sparsity of available in-situ measurements (Caton Harrison et al., 2022; Jones et al., 2016).

https://doi.org/10.5194/egusphere-2025-3374
Preprint. Discussion started: 8 September 2025

Broadly, most analysis found ERA5 performed better than, or as well as, other products when evaluated against in-situ observations. Li et al. (2013) found that ERA-Interim (a predecessor to ERA5) generally had a low bias in 10m wind speed compared to in-situ shipboard observations across the entire Southern Ocean (0.06 m s^{-1}, as compared to a high bias of 1.37 m s^{-1} for NCEP-DOE (the predecessor to NCEP-DOE2). When Jones et al. (2016) evaluated the ERA-Interim, JRA-55 (predecessor to JRA3Q), and MERRA1 (predecessor to MERRA2) reanalyses against research vessel observations, radiosonde automatic weather station (AWS) measurements, and radiosondes in the Amundsen sea, the group found that JRA-55 had the smallest biases in wind speed compared to AWS and research vessel observations, while ERA-Interim showed lowest biases when compared to radiosonde profiles. Overall, Jones et al. showed that all three products represented open-ocean wind speeds reasonably against observations. Caton Harrison et al. (2022) found ERA5 slightly outperformed JRA-55 and MERRA2 winds in an analysis against coastal station and Advanced Scatterometer (ASCAT) measurements, though performance was similar between reanalyses. Similarly, Dong et al. (2020) found ERA5 outperformed MERRA2, ERA-Interim, and JRA-55 against 56 meteorological stations over the Antarctic Ice Sheet. Li, Jones, and Caton Harrison all note that all reanalysis products overestimate in-situ winds at low-wind conditions (<~4 m s^{-1}) and underestimate them at high-wind conditions (>~25 m s^{-1}).

A global intercomparison of near-surface winds that included ERA5, MERRA2, R1, and JRA-55 (a predecessor of JRA3Q) found that ERA5 substantially outperformed the other reanalyses in reproducing in-situ observations from (land-based) tall tower platforms (Ramon et al., 2019). Based on these findings and the studies outlined above, we treat ERA5 as our benchmark reanalysis, following other Southern Ocean wind studies (e.g. Goyal et al., 2021).

2.2 Spatiotemporal Standardization

We account for differing spatial and temporal resolution when comparing reanalysis products (Table 1). 10-m wind speed calculated from u and v components at hourly resolution and then averaged to daily resolution is typically higher than wind speed calculated from the same u and v components that have been first averaged to daily resolution. We therefore average all u and v components to daily resolution before deriving wind speed. For similar reasons, we interpolate all three fields (u-component, v-component, and wind speed) to a standard 1°x1° grid using the cdo package (Schulzweida, 2023). We are interested primarily in the mean state, trends, and extremes of the open-ocean circumpolar winds. As the wind jet is typically found between -48°S and -54°S (Swart & Fyfe, 2012), we focus our analysis on the open water winds in the region 40°S to 60°S.

2.3 SAM index

https://doi.org/10.5194/egusphere-2025-3374
Preprint. Discussion started: 8 September 2025

In each reanalysis, we calculate and then evaluate the SAM index at monthly resolution against the observational SAM index (G. J. Marshall, 2003). Following Velasquez-Jimenez and Abram (2024), the "natural", or non-normalized, SAM index is calculated as:

SAM = P*40° S – P*65° S,

where P*40° S and P*65° S are the zonal MSLP anomalies at 40°S and 65°S, respectively, relative to the time period 1980-2019. In the observational SAM index, these MSLP anomalies are calculated from the mean of six station records near each of the two latitudes for which good long-term records exist. In the reanalysis SAM index we simply use the zonal mean at both latitudes. Compared to the more traditional SAM index (G. J. Marshall, 2003), the natural SAM index is not normalized by dividing by the reference interval standard deviation. It is therefore not dimensionless and given in units of hPa. This approach has the advantage of making the trends and magnitude of the index less sensitive to sampling frequency.

2.4 Modelled Ozone Depletion

We perform simulations with UKESM1 to quantify the relative contribution of ozone depletion and greenhouse gas induced warming on the wind field trends. UKESM is a well-established earth system model (ESM, Sellar et al., 2020; Yool et al., 2021) based on the HadGEM3-GC3.1 coupled physical atmosphere-ocean model (Kuhlbrodt et al., 2018). We refer readers to these articles for a general evaluation of UKESM1 and only highlight here components of the model that are central to our work. The atmospheric component of UKESM1 is the Global Atmosphere 7.1 (GA7.1) science configuration of the Unified Model (Walters et al., 2019), with horizontal resolution of approximately 135 km (1.25° × 1.875°), 85 vertical levels and a model top located at 85km altitude. Unusually for a CMIP6 (Coupled Model Intercomparison Project Phase 6; Eyring et al., 2016) model, UKESM1 simulates full atmosphere ozone chemistry through the U.K. Chemistry and Aerosols (UKCA) model (Archibald et al., 2020; Mulcahy et al., 2018), interactively coupled to the model's physics and dynamics. Ozone is therefore prognostic, with its evolution dependent on, and influencing, the simulated atmospheric thermal, dynamical and chemical states (Keeble et al., 2021).

The ability of UKESM1 to simulate the historical evolution of ozone has been discussed in Keeble et al. (2021). Of 22 models they analysed, only six interactively predicted stratospheric ozone, including UKESM1. UKESM1 overestimates the observed global mean total column ozone (TCO) over the period 1980 to 2015, but this overestimation is significantly reduced over the Antarctic region (60°S to 90°S). In addition, UKESM1 has a stronger negative TCO trend globally than observations, but this overestimate is again significantly reduced when the 60°S to 90°S region is considered (Keeble et al.,

https://doi.org/10.5194/egusphere-2025-3374
Preprint. Discussion started: 8 September 2025

2021). These biases should be kept in mind when the impact of ozone depletion and recovery on the surface physical climate is discussed.

2.5 Experimental Design

We control the evolution of stratospheric ozone in UKESM1 by modifying emissions of ozone depleting substances (ODS, e.g. CFCs and HCFCs), which play a central role in driving stratospheric ozone loss (Farman et al., 1985; Solomon et al., 1986). We perform simulations for 1950 to 2100 using two ODS emission scenarios: (i) ODS use the standard CMIP6 emissions (historical followed by a projection), and (ii) ODS are fixed at 1950 values. We refer to these two experiments as OZONE-HIST and OZONE-1950. OZONE-HIST results in ozone loss from approximately 1970 to 2000, followed by a slow recovery through to 2100 (Keeble et al. 2021, see their Fig 7). OZONE-1950 minimizes stratospheric ozone loss throughout the simulation as essentially no ODS reach the model stratosphere. The two ODS scenarios are combined with two CMIP6 SSP (shared socioeconomic pathway) scenarios (SSP 3-7.0 and SSP 1-2.6; Gidden et al., 2019) that represent a high and low GHG emission scenario. This configuration results in four experiments that allow us to isolate the effects of simulated stratospheric ozone and GHG on wind trends. Following McLandress et al. (2011), we assume that ozone-driven trends (resulting from the different ODS emissions) and GHG-driven trends are additive; that is, the OZONE-HIST run demonstrates a linear addition of ODS-driven trends and GHG-driven trends, so [OZONE-HIST – OZONE-1950] will isolate the ODS-driven trend, while any trends in the OZONE-1950 runs are due to GHG emissions alone.

These experiments are unique in that the ozone scenarios are internally generated by UKESM1, based solely on emissions of ODS. This means changes in atmospheric ODS impact the evolution of stratospheric ozone, and thus climate through the induced stratospheric ozone changes, as well as climate directly via the impact of changing ODS on infrared radiation. As a result, the impact of variable ODS is complete and internally consistent in our simulations. This differs from, for example CMIP6 DAMIP (Gillett et al., 2016), where simulations are run either with, or without, externally prescribed stratospheric ozone concentrations, which risk not being consistent with the host model's evolving thermodynamic, radiative, and chemical state.

For each UKESM1 experiment, we run three ensemble members, each branched in 1850 from the CMIP6 UKESM1 piControl following the procedure for generating initial conditions outlined in section 4 of Sellar et al., (2020). With respect to means and trends, we report the mean and trend of the ensemble mean value, calculated at daily 1°x1° resolution. When reporting extreme values, interannual variability, jet position, and standard deviation in the jet position, we calculate them for each ensemble member separately and give the mean of these calculations.

https://doi.org/10.5194/egusphere-2025-3374
Preprint. Discussion started: 8 September 2025

3. Results

3.1 Reanalysis Intercomparison

3.1.1 Wind climatology and distribution evaluation

We intercompare the reanalyses both to identify their utility for applications such as forcing ocean-only models, and to provide a baseline against which to evaluate the UKESM1 historical simulation. All the reanalysis products feature a prominent band of high winds between 40°S and 60°S, with intensification over the Indian Sector (Fig. 1). R1 strongly underestimates winds at high latitudes near the continent relative to the 1980-2019 ERA5 climatology but shows a less clear difference over the mid-latitude (40°S and 60° S) open ocean that varies zonally and averages to near-zero (Table 2-climatology). MERRA2 agrees with ERA5 at high latitudes but is evenly low compared to ERA5 over the open ocean. JRA3Q is relatively uniformly somewhat higher than ERA5 (Fig. 1).

The reanalysis products generally agree well when considering only the open-ocean winds between 40°S and 60°S. Most reanalyses are relatively similar to ERA5, ranging from a difference of -0.20 m s^{-1} (MERRA2) to 0.28 m s^{-1} (JRA3Q) for annual-average winds. In comparison, NCEP-DOE2, excluded from this analysis for high bias, has a bias of 1.31 m s^{-1} for yearly-averaged winds in the same region. Interannual variability (IAV) is relatively consistent but varies somewhat between reanalyses, ranging from 1.2% in ERA5 to 2.4%, or roughly double, in R1 (supplementary table (ST) 1). No strong seasonal differences in interannual variability are seen in any reanalysis.

The frequency distribution of the daily winds is remarkably similar between the reanalyses (Fig. 2, ST2), with differences mostly visible at the tails of the distribution. ERA5 has the lowest 'low' (5th percentile) winds, and R1 has somewhat anomalously high "low" winds (0.44 m s-1 higher than ERA5). The other reanalyses have 'low' winds only slightly (~0.1 m s^{-1}) higher than ERA5. There is more spread at the high end of the distribution, where ERA5 sits in the middle of the reanalysis set and year-round differences from ERA5 range from -0.35 m s^{-1} (MERRA2) to 0.59 m s^{-1} (JRA3Q).

3.1.2 Wind speed trends

Trends in open-ocean wind speed differ between the reanalyses much more than the climatological mean fields (Fig. 2a-b, Fig. 3, Table 3). JRA3Q and ERA5 behave similarly over the whole time period (1980-2019), having a statistically significant year-round mean trend of ~0.04 m s^{-1} dec^{-1} that is slightly stronger in austral summer and autumn and

https://doi.org/10.5194/egusphere-2025-3374
Preprint. Discussion started: 8 September 2025

not statistically significant in winter (JJA) and spring (SON). In contrast, R1 and MERRA2 have much stronger trends – ~3.5x and ~2.5x the magnitude of the ERA5 annual mean trend, respectively. The seasonality in these two reanalyses is also very different from ERA5, with relatively strong, statistically significant trends persisting year round. Trends in R1 and MERRA2 are also statistically significant over a much larger area of the Southern Ocean, as well as in the JJA season (Fig. 3).

Summer (DJF) mean wind speed trends in the period of maximum ozone depletion (1980-1999) are approximately double those for the full time period in all reanalyses (Fig. 2, Table 3). Trends in the extreme winds follow a similar pattern to the mean winds, with R1 and MERRA2 trends much stronger than those of JRA3Q and ERA5 (Fig. 2, e)-h)). Trends in extreme winds are not systematically stronger than trends in mean winds and are less likely to be statistically significant.

3.1.3 Jet position and poleward trend

The annual average zonal mean wind jet sits at -52.1°S in ERA5 and is similar between products, ranging from -51.6°S (R1) to -52.3°S (JRA3Q) (Fig. 4, ST3). The jet position exhibits a substantial seasonal cycle, being at its most southerly location in austral autumn and most northerly location in austral spring. All reanalyses represent this seasonal cycle in the jet position, which ranges in amplitude (of the seasonal averages) from ~1.6° (MERRA2) to ~2.4° (R1). Interannual variability of the mean jet position over the time period 1980-2019 is comparable between reanalyses – the standard deviation of the zonal mean ranges from 0.8° (MERRA2) to 0.9° (R1). The zonally-varying standard deviation of the jet position (shown in Fig. 4 only for ERA5, for clarity) is also comparable. The strongest poleward trend in the wind jet occurs in austral summer and autumn, and is much stronger (1.8x – 3.8x) during the period of maximum ozone depletion (1980-1999) than over the whole time period (ST4). Trends in the position of the jet are not always statistically significant in the reanalyses because of the large interannual variability.

3.1.4 SAM index

The timeseries of the station-based SAM index (see Methods) provides a possible observational constraint on the accuracy of the reanalysis products. The SAM indices derived from reanalyses exhibit a high temporal coherence with the observational SAM index, with some deviations – for example in JRA3Q during 2005-2010 (Fig. 5). The trend in the SAM index has a seasonal character both in the observations and in the reanalyses. It is strongest in austral summer (DJF) and autumn (MAM), and typically much weaker and not statistically significant in the other seasons (Fig. 5, ST5). The observational trend is much stronger in the period of maximum ozone loss than in the whole time period (factor of ~3x), which is reflected in the reanalyses (factor of ~2.3-3.6x).

https://doi.org/10.5194/egusphere-2025-3374
Preprint. Discussion started: 8 September 2025

In all seasons, the trend in the SAM index in the reanalyses correlates tightly with the trend in the estimated wind speed ($r=0.72$-0.93, $p<0.05$). Because the wind acceleration is mechanistically linked to the trend in the SAM, evaluating the accuracy of the reanalysis-derived SAM indices against the observational index could potentially provide a constraint on the accuracy of reanalyzed wind speed trends; i.e. a trend in the SAM should result in a trend in the wind speed.

Notably, this observational SAM constraint suggests that the strong trends in the R1 and MERRA2 reanalyses in austral winter and spring over the period of maximum ozone depletion may be spurious, as they are accompanied by strong SAM index trends that are not present in the observations (Fig. 5, panels d and e). Additionally, in autumn, the ERA5 and JRA3Q time series appear to underestimate the SAM trend during 1980-1999, while R1 and MERRA2 overestimate it over the course of the whole time series, suggesting possible corresponding overestimations/underestimations of the respective wind trends. In summer, the observational constraint appears to have less power, as the reanalyses show a variety of wind speed trends while all representing the SAM relatively accurately (Fig. 5b).

3.1.5 Reanalysis intercomparison summary

Overall, all four reanalyses show relative coherence in mean wind speed climatology, distribution, jet position and jet seasonal cycle. Moderate differences in extreme winds, interannual variability and jet latitudinal trend are observed. Reanalyses tend to exhibit systematic biases in capturing the tails of the observational wind distribution (i.e., they overestimate extremely low winds and overestimate extremely high winds relative to observations; see summary of previous in-situ evaluation in Methods). Thus, it is plausible that ERA5, which has the lowest extreme low winds, is the best representation of the low tail of the distribution, while JRA3Q may be the best at representing high winds.

The most important differences between the reanalysis products are in the representation of the wind speed trends over the time period 1980-2019. R1 and MERRA2 have considerably stronger trends than ERA5 and JRA3Q, and moreover these trends persist year round. To evaluate which trends seem more plausible, we consider an observational constraint in the form of the observational SAM index. R1 and MERRA2 appear to overestimate SAM index trends, especially in austral winter and spring, suggesting that their strong wind trends in these time periods may be spurious. This provides additional rationale for using ERA5 as the baseline reanalysis against which to evaluate the UKESM1 model at southern high latitudes.

3.2 UKESM1 evaluation against reanalyses

https://doi.org/10.5194/egusphere-2025-3374
Preprint. Discussion started: 8 September 2025

We next evaluate the main Southern Ocean wind features in UKESM1 against our default reanalysis, ERA5, to assess the model's suitability for answering scientific questions related to changing wind patterns in this region. The UKESM1 model has an overall year-average positive bias of ~0.3 m s^{-1} relative to the ERA5 climatology in the band between 40°S and 60°S (Fig. 1), which does not vary substantially by season (Table 2). UKESM1 underestimates winds at high latitudes compared to ERA5 while showing the strongest positive bias over the mid-latitude open ocean. However, on average, the UKESM1 distribution is similar to that of ERA5, though slightly shifted towards higher winds than the reanalyses in the middle of the distribution (Fig. 2). Extreme low (5th percentile) winds are nearly identical to ERA5 values, while the highest winds are somewhat higher (~0.3 m s^{-1}, ST2). Interannual variability in UKESM1 is comparable to that of ERA5, with an average ratio of 0.8 (IAV_{UKESM1}/IAV_{ERA5}) for annual values (ST1).

UKESM1 has similar decadal trends in wind speed as ERA5, with strongest acceleration in austral summer (0.04 and 0.06 s-1 dec-1 for for UKESM1 and ERA5, respectively, over 1980-2019, as compared to to 0.11 and 0.14 s^{-1} dec^{-1} over 1980-1999; Table 3). The general pattern of significant wind trend strength peaking in austral summer is consistent between the model and ERA5. Spatial patterns (significant acceleration occurring mostly in the 40-60°S band, and more visible in austral summer, Fig. 3), are also reproduced by the model.

The UKESM1 jet position is similar to that of ERA5 (Fig. 4, ST3) and accurately captures the observed seasonal cycle in position (most southerly in MAM, most northerly in SON). The majority of the temporal variability in jet location is a result of natural variability (as opposed to from a forced signal, such as ozone depletion). We would therefore not expect a free running coupled model like UKESM1 to capture the temporal evolution of this variability. (We would, however, expect the model to capture any externally forced, longer-term trends.) The magnitude of variability in the jet location is comparable between UKESM1 and ERA5, as seen in the zonally-varying standard deviation for 1980-2019 (Fig 4), indicating UKESM accurately represents natural variability signals in this region. The UKESM1 trends in the poleward position of the jet are much stronger than in the reanalyses over the whole time period (~1.8x ERA5 in the annual mean, ~1.7x ERA5 in the DJF mean, ST4), a feature that is amplified in the period of maximum ozone loss (1980-1999, ST4). This feature may be due to ozone loss in UKESM1, in response to ODS emissions, being somewhat higher than seen in observations (Keeble et al., 2021).

The variability and trend in the SAM index is comparable to that of ERA5 and the observations (Fig. 5, ST5). As in the case with the jet position, UKESM1 does not reproduce the time variation in the SAM index seen in the reanalyses because of the significant role natural variability plays in the temporal evolution of the SAM index. Trends in the SAM index during 1980-1999 are much (up to ~3x) stronger than those during 1980-2019, both in the ERA5 reanalysis and in UKESM1. Similarly to ERA5 and JRA3Q, in both time periods, UKESM1 has strongest, most significant SAM trends during DJF and MAM, accompanied by stronger wind acceleration in those seasons (Fig. 5). In particular, UKESM1

https://doi.org/10.5194/egusphere-2025-3374
Preprint. Discussion started: 8 September 2025

accurately captures the SAM trend in DJF, including the differential trends between the full period and the shorter 1980-1999 period. This differential response is less accurately captured in MAM, although the SAM trend for the full period is well simulated.

Overall, the representation of UKESM Southern Ocean wind climatology and distribution, including extremes, as well as decadal trends and trends in the SAM index, is remarkably consistent with that of ERA5; however, mean wind speeds are somewhat higher in the model. The mean jet position is also preserved, though UKESM1 demonstrates stronger poleward movement than all reanalyses. As a result of its accurate representation of wind trends, we suggest UKESM1 can be used to understand forced wind regime changes in this region, both in the past and in the future. Furthermore, the model is suitable as a dataset for forcing offline ocean models for studying the Southern Ocean carbon and heat cycles.

3.3 Attribution of wind speed trends to GHG emissions and ozone depletion

We finally use UKESM1 to attribute past, and potential future, changes in the Southern Hemisphere wind regimes to either stratospheric ozone changes or greenhouse gas forcing. We do this by combining two ODS scenarios (ODS-HIST and ODS-1950) with two CMIP6 emission scenarios: SSP 1-2.6 and SSP 3-7.0 for the period 1950 to 2100 (see Methods). For each experiment, we show all three model ensemble members, as well as the ensemble mean.

Over the full time period, winds increase in all seasons and scenarios (Fig. 6). The most prominent feature in the time series is a steep wind acceleration in the scenario with historical ozone depletion (OZONE-HIST), approximately during 1980-2000, occurring predominantly in austral summer and to a minor extent in austral spring (Fig. 6). During the same time period, no acceleration – in fact, a minor slowdown is seen in the scenario without ozone depletion (ST6). We first partition the attribution of the observed historical wind changes to greenhouse gas emissions and ozone depletion, comparing them with those seen in ERA5, and then consider potential changes over the 21st century, again attributing changes to ozone forcing and/or greenhouse gas emissions.

UKESM1 exhibits the same positive relationship between the trend in the SAM index and wind speed that was seen in the reanalyses. Wind acceleration (deceleration) corresponds to a positive (negative trend) in the SAM index in all ensemble members of the two experiments over the historical period (Fig. 7). Remarkably, though absolute wind speeds are higher in UKESM1 than in the ERA5 reanalysis, the trend magnitudes for both periods are very similar in both datasets in all seasons (Fig. 7, Table 3), suggesting that the forced signal of ozone depletion in UKESM1 captures real-world dynamics.

https://doi.org/10.5194/egusphere-2025-3374
Preprint. Discussion started: 8 September 2025

The key role of ozone in driving the historical SAM and wind speed changes becomes further apparent when comparing the OZONE-HIST and OZONE-1950 runs: all three ensemble members of the OZONE-1950 experiment show a much weaker wind speed trend over the whole time period (Fig. 7, filled green squares) and a negative trend over the period of maximum ozone depletion (empty green squares). Meanwhile, the OZONE-HIST runs (black squares) agree with both ERA5 and the observational SAM index over both the whole time period (filled black squares) and the period of maximum ozone depletion (empty black squares).

The general congruence of the historical UKESM1 runs with ERA5 suggests that UKESM1 captures both the sensitivity of the wind and SAM response to the time-varying trend in the ozone forcing, as well as the seasonality of this response. Both wind and SAM trends are stronger over the period of maximum ozone depletion than over the full time period, and changes in the austral summer mean are larger than in the annual mean, with minimal changes in austral winter. This congruence is especially notable because UKESM1's ozone chemistry is fully interactive (as opposed to the more common case of models having prescribed atmospheric ozone concentrations), so the model's accurate wind and SAM trends suggest it successfully reproduces both the response of ozone to changing ozone-depleting emissions and the dynamical wind response to changes in ozone.

We next attribute the wind changes throughout the whole simulation period 1950-2100 to either ozone or GHG forcing, subdividing the time series into three 50-year periods. In the latter half of the 20th century (1950-1999; Table 4), winds accelerated in all seasons but most strongly in DJF, followed by SON. This acceleration was driven entirely by ozone loss; winds actually slowed down slightly over 1950-2000 in the OZONE-1950 run, in all seasons except SON (Table 4).

In the first half of the 21st century (2000-2049), in the realistic (ODS-HIST) runs, winds stay approximately constant in most seasons in both SSP scenarios, though they accelerate significantly in austral winter (Fig. 7, Table 4). This lack of trend is actually due to the (accelerating) GHG effect counteracting the (decelerating) ozone recovery effect, which can be seen when decomposing the overall signal into the two forcing factors (Table 4). Though the acceleration due to GHG is stronger under the higher-emissions (SSP 3-7.0) scenario, the effect of ozone recovery is also stronger under this scenario and the two effects cancel out (Table 4). The overall acceleration seen in austral winter (JJA) is a result of the different seasonalities of the two forcing factors: while ozone depletion and recovery is predominantly a summer phenomenon, these model simulations show that GHG-driven wind acceleration is strongest in winter, resulting in an unbalanced GHG forcing of wind trends during austral winter.

Finally, in the latter half of the 21st century (2050-2099), the simulations show a difference in wind trends based on GHG emission level. Under SSP 1-2.6 with historical ozone recovery, wind speed stagnates in all seasons, while under SSP

https://doi.org/10.5194/egusphere-2025-3374
Preprint. Discussion started: 8 September 2025

3-7.0, winds accelerate in austral winter and spring, both with and without ozone depletion (Fig. 7). However, these trends are typically not statistically significant, due to large interannual variability.

4. Discussion and Conclusions

The main aims of this work were to evaluate the representation of recent-past Southern Ocean winds in the most commonly used contemporary reanalysis products, to evaluate their representation in a free-running Earth system model (UKESM1), and finally to use this model to attribute drivers of changes in these winds both over the recent past and through to 2100. The initial intercomparison of the reanalyses shows that, while the general features of the Southern Ocean winds (mean, distribution, jet location, and extremes) are relatively congruent, the reanalyses vary considerably in wind speed trends. In all reanalyses, trends are strongest in the period of maximum ozone depletion (1980-1999), and comparatively strongest in austral summer, consistent with the existing understanding of forcing due to ozone loss, which is primarily a summer phenomenon. However, trends in MERRA and R1 are comparatively much stronger and tend to persist year-round, while trends in ERA5 and JRA3Q are weaker and concentrated in austral summer.

We assess which trend representation is more realistic using a novel observational constraint: we compare trends in the observational SAM index to their representation in the reanalyses, and then relate them to wind speed trends. Because a positive (negative) SAM index trend is mechanistically linked to a positive (negative) wind trend, performance in one metric may imply performance in the other. Applying this constraint suggests the high winter trends seen in winter and spring in the MERRA and R1 reanalyses may be spurious, as they are accompanied by strong SAM trends that are not seen in the observational record. Thus, we conclude that ERA5 and JRA3Q are best suited for studies of wind and SAM changes in this region, as well as for forcing ocean models.

Evaluation of UKESM1 winds and SAM index against the baseline reanalysis (ERA5) suggests UKESM1 is well suited to study wind changes over the Southern Ocean, or to force offline oceanographic models for this purpose. Notably, UKESM1 performs well in reproducing the intensity distribution of daily wind speeds and tails of ERA5, though the overall mean of the distribution is somewhat higher in UKESM1 (~0.3 m s-1). UKESM also reproduces the ERA5 historical decadal trends in both the winds and the SAM index, including the differential response between the 1980-2000 period and the full 40 year period, indicating correct sensitivity of winds to ozone changes. The seasonality of the SAM and wind trends is also well reproduced, with strongest trends in austral summer. However, the poleward jet trend is stronger in UKESM1 than in any of the reanalyses, somewhat in contrast to the correctly reproduced behaviour of the other metrics.

https://doi.org/10.5194/egusphere-2025-3374
Preprint. Discussion started: 8 September 2025

Using future projections made with UKESM1, with and without ozone depletion, we then attribute the observed changes to the relative influence of ozone depletion and greenhouse gas emissions, both historically over 1980-2020 and as projected by the model to the end of the 21st century. The UKESM1 simulations show the observed acceleration of winds in the latter half of the 20th century is entirely attributable to ozone depletion. In the first half of the 21st century, summer winds stagnate, as wind slowdown due to ozone recovery competes with wind acceleration due to persistent GHG emissions. In contrast, winds accelerate in austral winter and spring, as the GHG effect outcompetes the ozone recovery effect, which is predominantly a summer phenomenon and not strong in these seasons. In the latter half of the 21st century, a more clear bifurcation between wind trends under the low and high SSP scenario is visible, especially in austral winter and spring. Winds accelerate more under the high SSP scenario, while stagnating under the low SSP scenario. In this time period, the role of ozone recovery is minor.

We show that ozone depletion overwhelmingly drove the observed summer wind acceleration in the latter half of the 20th century, and we expect this trend to reverse in the first half of the 21st century. By the second half of the 21st century, greenhouse gas loading is the main factor driving wind changes, with more emissions leading to more acceleration, but it is strongly active only in austral winter and spring. Thus, we demonstrate a shift in the dynamical controls on the wind behaviour over the Southern Ocean from ozone in the latter half of the 20th century to greenhouse gas emissions in the latter half of the 21st century. This control shift is consistent with the general understanding; Polvani et al. (2011), Arblaster et al. (2011), McLandress et al (2011), Solomon et al (2017), and others discuss this decreasing importance of ozone to atmospheric circulation as the ozone hole heals. Our work here, which focuses on the near-surface winds, extends this understanding by providing a constrained estimate of the changing surface wind speed trends in response to this shift, based on a model with interactive chemistry whose past performance is validated against both reanalyses and the observational SAM index.

To first order, a future increase in wind intensity due to GHG loading would act to strengthen the meridional overturning circulation and the ACC, both of which may support increased heat uptake by the Southern Ocean (Morrison et al., 2015). However, the magnitude of the overturning and ACC responses to changes in wind intensity is disputed, and depends on the magnitude of eddy compensation and the role of buoyancy forcing (e.g. Morrison et al. 2011, Bishop et al., 2016; Shi et al., 2020). Recent work has even suggested a strong slowdown of the ACC in response to GHG emissions, driven by increased surface freshening from the melt of ice shelves around Antarctica (Sohail et al., 2025). The ultimate effect of GHG loading on the circulation of the Southern Ocean remains an open question, implying uncertainty in heat uptake. In contrast, the rate of future Southern Ocean carbon uptake may be relatively insensitive to potential changes in regional circulation as the surface-depth gradient in ocean carbon diminishes and may instead be dominated by temperature changes (Jarníková et al., 2025).

https://doi.org/10.5194/egusphere-2025-3374
Preprint. Discussion started: 8 September 2025

Code and data availability

Code and data are provided on DRYAD: {to be finalized if accepted}. For convenience, analysis code is also at https://github.com/tjarnikova/windEval.

Author contribution

Conceptualization: T.J., C.J., and C.L.Q. Methodology: C.J., T.J., S.R., and C.L.Q. Investigation: T.J. Visualization: T.J. Funding acquisition: C.L.Q. and C.J. Project administration: C.L.Q. Supervision: C.J. and C.L.Q. Writing—original draft: T.J. Formal analysis: T.J Software: T.J. and S.R. Data curation: T.J. Validation: T.J., S.R., and C.L.Q. Writing—review and editing: C.J., T.J., and C.L.Q.

Competing interests

The authors declare that they have no conflict of interest.

Acknowledgements

We thank all people who contributed to the development of the UKESM1 model and the atmospheric reanalyses used in this analysis, and the Research and Specialist Computing Support service of the High Performance Computing Cluster at the University of East Anglia.

Funding

U. K. Natural Environment Research Council CELOS project (grant NE/T01086X/1) (CJ, CLQ)
U. K. Natural Environment Research Council TerraFIRMA: Future Impacts, Risks and Mitigation Actions in a changing Earth System project, (grant NE/W004895/1) (CJ, SR)
U.K. Royal Society (grant RSRP\R\241002) (CLQ)

https://doi.org/10.5194/egusphere-2025-3374
Preprint. Discussion started: 8 September 2025

Figures and tables

Table 1

Name	ERA5	JRA3Q	MERRA2	R1
Institution	ECMWF	JMA	NASA GMAO	NOAA/NCEP and NCAR
Period coverage	1940 to present	1947 to present	1980 to present	1948 to present
Time resolution	1-hr	6-hr	1-hr	6-hr
Horizontal grid (lat. × lon.)	0.25° × 0.25°	0.37°× 0.37°	0.5°× 0.625°	1.875° × 2°
Reference	Hersbach et al., 2020	Kosaka et al., 2024	Molod et al., 2015	Kalnay et al., 2018

Table 1: Basic characteristics of the reanalysis products used.

https://doi.org/10.5194/egusphere-2025-3374
Preprint. Discussion started: 8 September 2025

Fig. 1

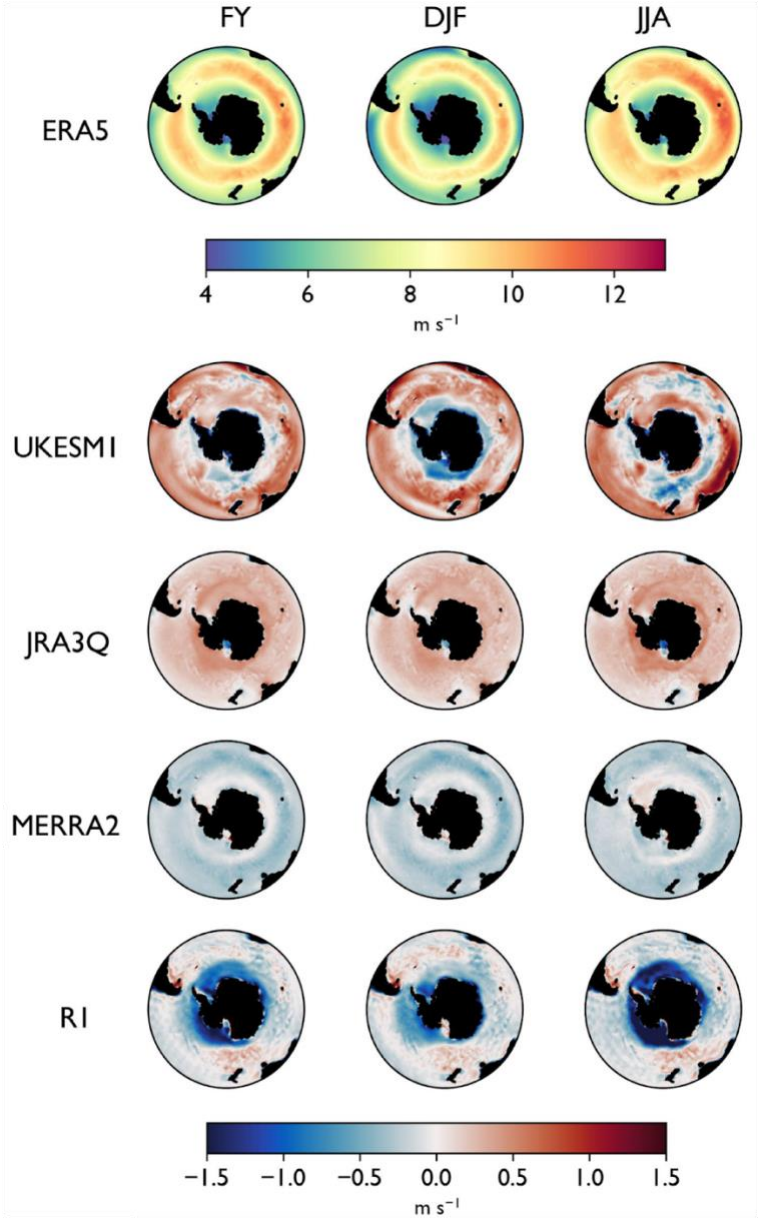

Fig. 1: Climatological wind speed. *For ERA5, the climatological wind speed for the full year and austral summer (DJF) and winter (JJA) is shown. For the other 3 reanalyses and UKESM1, differences from ERA5 are shown as [product x – ERA5]; i.e. positive (red) values indicate higher winds than ERA5. See also Table 2.*

https://doi.org/10.5194/egusphere-2025-3374
Preprint. Discussion started: 8 September 2025

Fig. 2

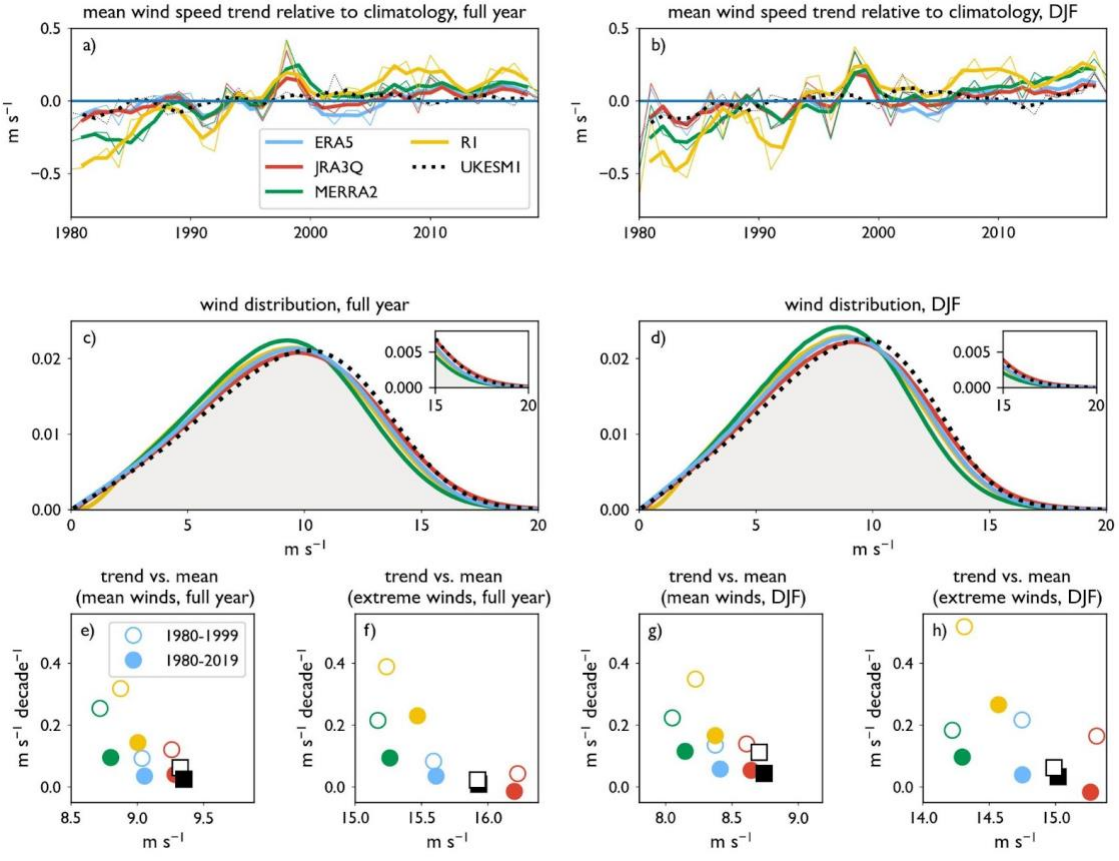

Fig. 2: Summary statistics for wind distributions in four reanalysis products and UKESM1. *a-b): mean wind speed trends relative to climatology for a) full year and b) DJF only. Thick lines have been smoothed by a three-point running filter. c-d): windspeed frequency distribution (100 bins, 0-20 m s⁻¹) for c) full year and d) DJF, with high tails shown in inset. e-h) Trends in mean and extreme winds for full year and DJF vs. climatological means, with colours the same as in panel a). Filled symbols represent 1980-2019, while open symbols represent 1980-1999; circles represent reanalyses while squares represent UKESM1. Colours from panel a) are repeated throughout the figure. Summary statistics shown in panels e)-h) are also given in Tables 2 and 3. All figure statistics are calculated for daily winds at 1°x1° resolution, 40°S- 60°S.*

https://doi.org/10.5194/egusphere-2025-3374
Preprint. Discussion started: 8 September 2025

Table 2

climatological wind speed, m s^{-1}, 1980-2019					
	ERA5	**R1**	**MERRA2**	**JRA3Q**	**UKESM1**
full year	9.05	-0.05	-0.20	0.28	0.30
DJF	8.41	-0.04	-0.23	0.27	0.33
MAM	9.13	-0.02	-0.28	0.24	0.36
JJA	9.5	-0.08	-0.13	0.31	0.19
SON	9.16	-0.07	-0.18	0.31	0.32

Table 2: Climatological wind speed. *Seasonally subdivided open-ocean wind speed between 40°S and 60° S for ERA5 (1980-2019), and differences from ERA5 for the other reanalyses and UKESM1.*

https://doi.org/10.5194/egusphere-2025-3374
Preprint. Discussion started: 8 September 2025

525 Fig. 3

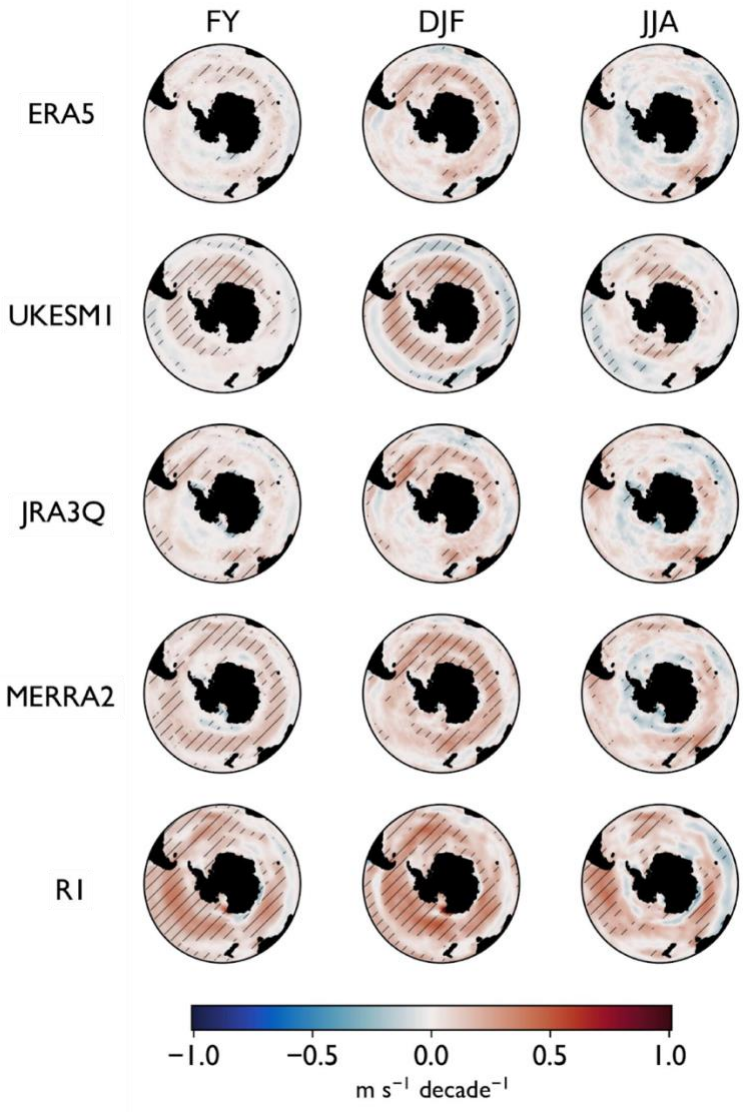

Fig. 3: Decadal trends in wind speed (1980-2019). *Hatching shows trends significant at the 95% confidence level. See also Table 3.*

530

https://doi.org/10.5194/egusphere-2025-3374
Preprint. Discussion started: 8 September 2025

Table 3

trend in wind speed, m s^{-1} $decade^{-1}$, 1980-2019					
	ERA5	R1	MERRA2	JRA3Q	UKESM1
full year	**0.04**	**0.14**	**0.10**	**0.04**	**0.03**
DJF	**0.06**	**0.17**	**0.12**	**0.05**	**0.04**
MAM	**0.05**	**0.17**	**0.13**	**0.06**	0.02
JJA	0.02	**0.13**	**0.08**	0.03	0.02
SON	0.01	**0.11**	**0.06**	0.02	0.02
trend in wind speed, m s^{-1} $decade^{-1}$, 1980-1999					
full year	**0.09**	**0.32**	**0.26**	**0.12**	**0.06**
DJF	**0.14**	**0.35**	**0.22**	**0.14**	**0.11**
MAM	0.09	**0.31**	**0.26**	**0.14**	0.02
JJA	0.08	**0.30**	**0.28**	0.12	**0.08**
SON	0.07	**0.31**	**0.25**	0.09	0.04

Table 3: Decadal trends in wind speed. *Seasonally subdivided trends in open-ocean wind speed between 40°S and 60° S are shown for 1980-2019 and 1980-1999. Trends significant at the 5% level are given in bold.*

https://doi.org/10.5194/egusphere-2025-3374
Preprint. Discussion started: 8 September 2025

Fig. 4

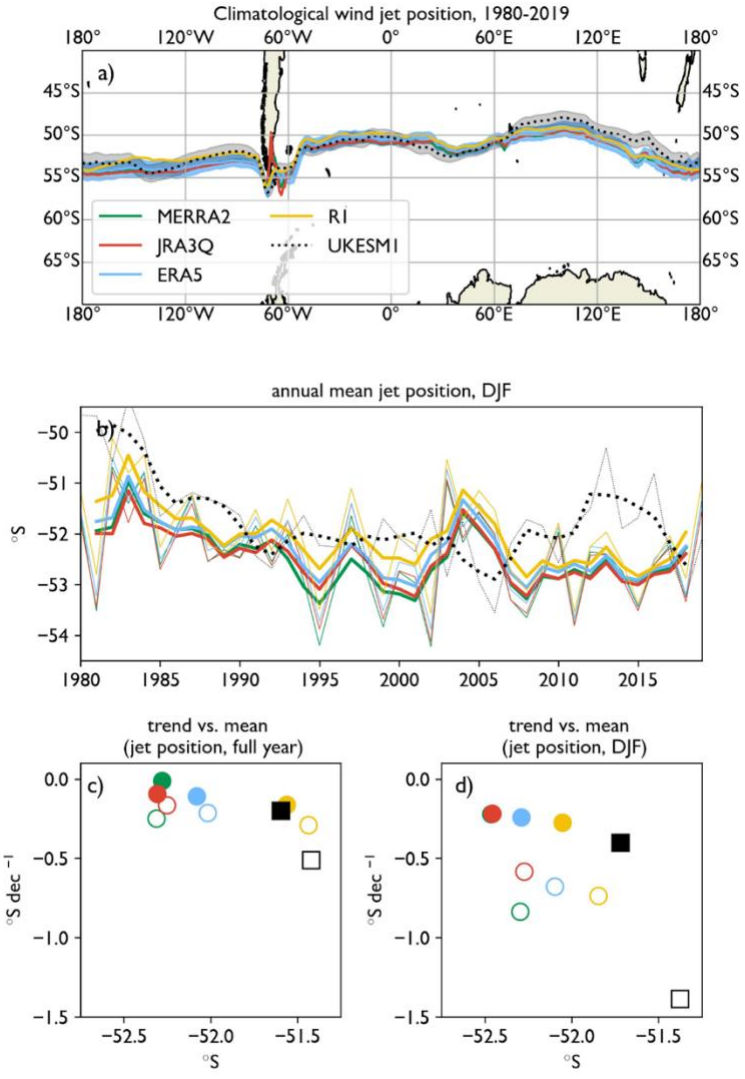

Fig. 4: Summary statistics for the wind jet. *a): the climatological mean annual jet position, with one standard deviation of the annual mean shown for ERA5 and UKESM1. b): The zonal mean of the austral summer jet position. Thick lines indicate smoothing by a 3-point running mean filter. c-d): Trends in the annual (c) and summer (d) jet position mean vs. climatological means. Colours from panel a) are repeated throughout the figure. See also Sup. Tables 3 and 4.*

https://doi.org/10.5194/egusphere-2025-3374
Preprint. Discussion started: 8 September 2025

Fig. 5

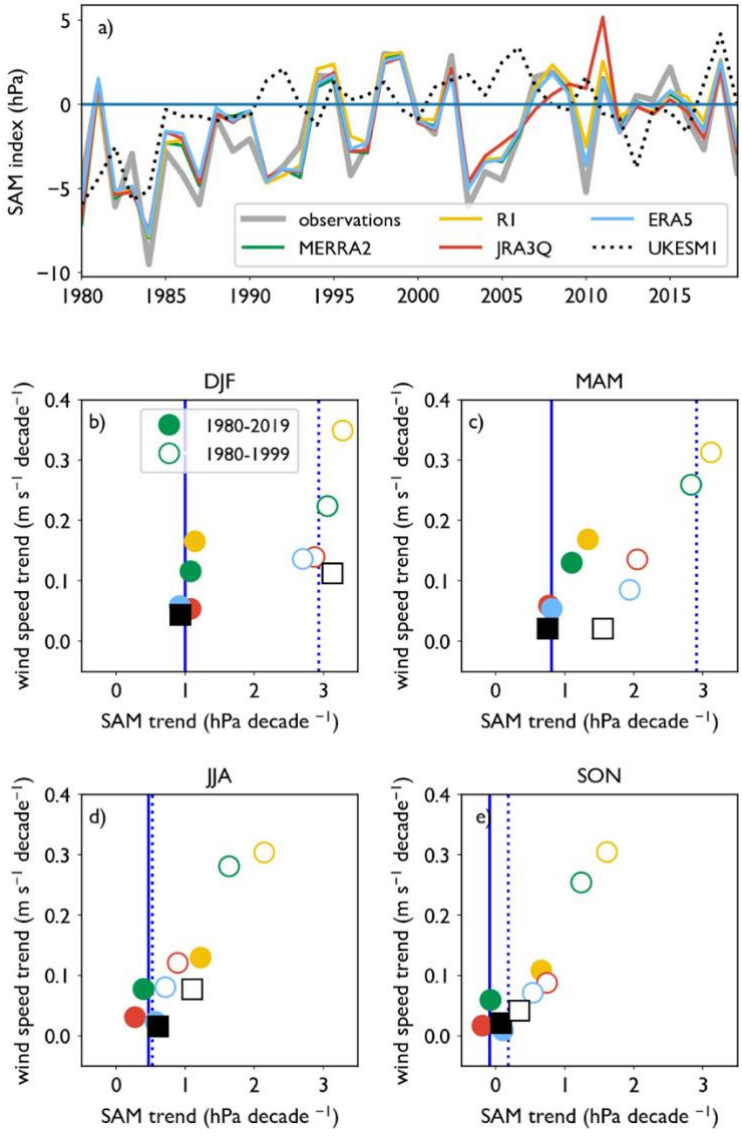

Fig. 5: Summary statistics for the SAM index. *a) Timeseries of the austral summer (DJF) SAM index. To highlight coherence of interannual variability, no running-mean filter has been applied. b-e) Trends in the wind speed vs trends in the SAM index, subdivided by season. Filled symbols represent 1980-2019, while open symbols represent 1980-1999. Vertical lines show the observational SAM index (full line represents 1980-2019, dotted line represents 1980-1999). Colours from panel a) are repeated throughout the figure. See also Sup. Table 5.*

https://doi.org/10.5194/egusphere-2025-3374
Preprint. Discussion started: 8 September 2025

Fig. 6

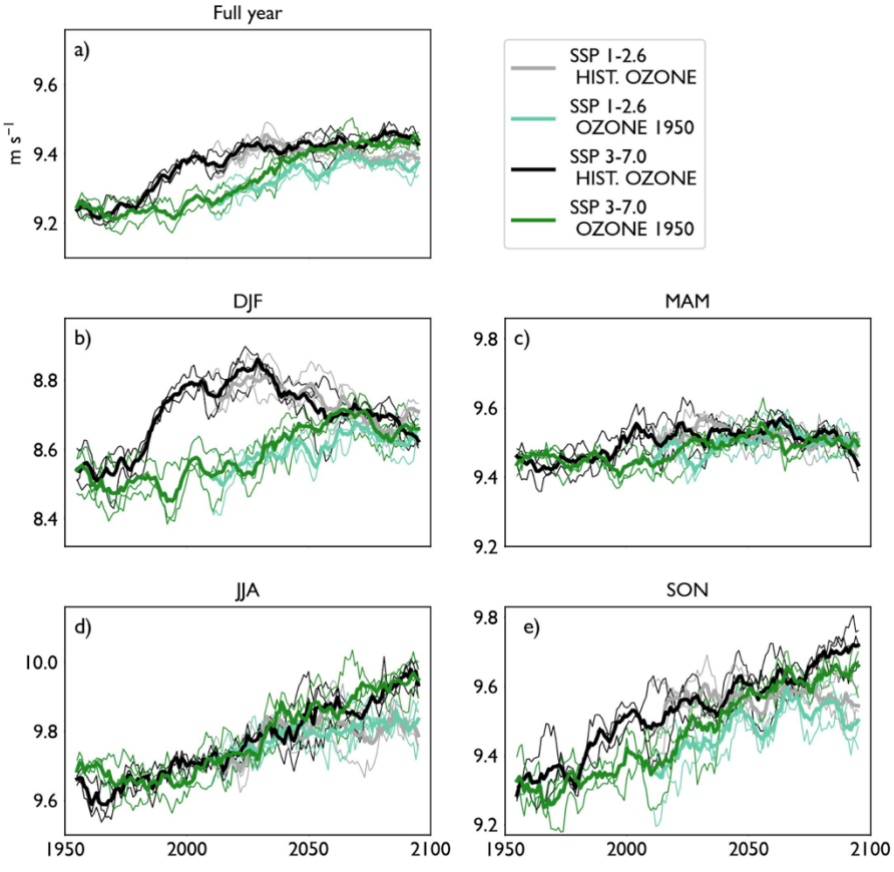

Fig. 6: Wind speed evolution from 1950 to 2100 in the OZONE-1950 and OZONE-HIST experiments. *a) Full year, b-e): seasonally subdivided means. All means are calculated for daily winds at 1°x1° resolution, 40°S-60°S. For each experiment, three ensemble members are shown, with the ensemble mean shown in bold. All lines are smoothed with a 10-year running filter. See also Table 4.*

https://doi.org/10.5194/egusphere-2025-3374
Preprint. Discussion started: 8 September 2025

Fig. 7

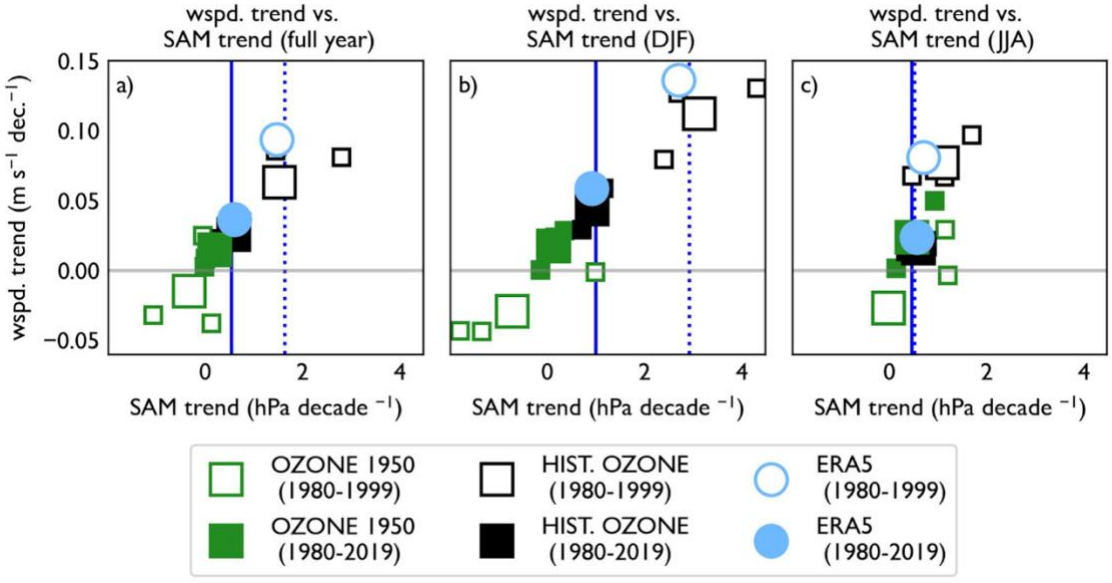

Fig. 7: Trends in mean wind speed vs. trends in the SAM index for the OZONE-1950 and OZONE-HIST experiments. *ERA5 is shown for comparison (blue circles), and the observational SAM index is shown as vertical lines (full for 1980-2019, dotted for 1980-1999). For the OZONE-1950 and OZONE-HIST experiments, individual ensemble members are shown as smaller squares, while the ensemble mean is shown as a larger square. As in Figs. 2,4, and 5, filled symbols represent 1980-2019, while open symbols represent 1980-1999.*

https://doi.org/10.5194/egusphere-2025-3374
Preprint. Discussion started: 8 September 2025

Table 4

1950-1999	GHG + ozone	GHG only	ozone only
FY	**0.03**	-0.01	**0.04**
DJF	**0.06**	-0.02	**0.07**
MAM	0.01	0.00	0.01
JJA	0.02	-0.01	**0.03**
SON	**0.04**	0.01	**0.03**

	SSP1-2.6			SSP3-7.0		
2000-2049	GHG + ozone	GHG only	ozone only	GHG + ozone	GHG only	ozone only
FY	**0.01**	**0.02**	-0.01	**0.01**	**0.03**	**-0.02**
DJF	0.00	0.01	-0.01	0.00	**0.02**	**-0.03**
MAM	0.00	0.01	-0.01	0.00	**0.02**	**-0.02**
JJA	**0.03**	**0.03**	0.00	**0.03**	**0.04**	-0.01
SON	0.02	**0.03**	-0.01	**0.02**	**0.04**	-0.02

	SSP1-2.6			SSP3-7.0		
2050-2099	GHG + ozone	GHG only	ozone only	GHG + ozone	GHG only	ozone only
FY	-0.01	0.01	-0.01	0.00	0.01	0.00
DJF	**-0.02**	0.01	**-0.03**	**-0.02**	-0.01	-0.01
MAM	0.00	-0.01	0.00	**-0.02**	-0.01	-0.01
JJA	-0.01	0.01	-0.02	0.02	**0.02**	0.00
SON	0.00	0.01	-0.01	**0.03**	**0.02**	0.01

Table 4: Attribution of wind trends (m s^{-1} dec^{-1}) to GHG and ozone forcing in three 50-year time-periods in the UKESM1 model runs. *Values for GHG + ozone refer to the ensemble mean trend of the OZONE-HIST run, while the GHG only column refers to the OZONE-1950 run. The effect of ozone only is then obtained by subtracting OZONE-1950 from OZONE-HIST. Statistically significant trends are given in bold.*

https://doi.org/10.5194/egusphere-2025-3374
Preprint. Discussion started: 8 September 2025

References

Arblaster, J. M., Meehl, G. A., & Karoly, D. J. (2011). Future climate change in the Southern Hemisphere: Competing effects of ozone and greenhouse gases: SH CLIMATE CHANGE-OZONE VERSUS GHGS. *Geophysical Research Letters*, *38*(2). https://doi.org/10.1029/2010GL045384

Archibald, A. T., O'Connor, F. M., Abraham, N. L., Archer-Nicholls, S., Chipperfield, M. P., Dalvi, M., Folberth, G. A., Dennison, F., Dhomse, S. S., Griffiths, P. T., Hardacre, C., Hewitt, A. J., Hill, R. S., Johnson, C. E., Keeble, J., Köhler, M. O., Morgenstern, O., Mulcahy, J. P., Ordóñez, C., … Zeng, G. (2020). Description and evaluation of the UKCA stratosphere–troposphere chemistry scheme (StratTrop vn 1.0) implemented in UKESM1. *Geoscientific Model Development*, *13*(3), 1223–1266. https://doi.org/10.5194/gmd-13-1223-2020

Bishop, S. P., Gent, P. R., Bryan, F. O., Thompson, A. F., Long, M. C., & Abernathey, R. (2016). Southern Ocean Overturning Compensation in an Eddy-Resolving Climate Simulation. *Journal of Physical Oceanography*, *46*(5), 1575–1592. https://doi.org/10.1175/JPO-D-15-0177.1

Bracegirdle, T. J., Shuckburgh, E., Sallee, J.-B., Wang, Z., Meijers, A. J. S., Bruneau, N., Phillips, T., & Wilcox, L. J. (2013). Assessment of surface winds over the Atlantic, Indian, and Pacific Ocean sectors of the Southern Ocean in CMIP5 models: Historical bias, forcing response, and state dependence: CMIP5 SOUTHERN OCEAN SURFACE WINDS. *Journal of Geophysical Research: Atmospheres*, *118*(2), 547–562. https://doi.org/10.1002/jgrd.50153

Caton Harrison, T., Biri, S., Bracegirdle, T. J., King, J. C., Kent, E. C., Vignon, É., & Turner, J. (2022). Reanalysis representation of low-level winds in the Antarctic near-coastal region [Preprint]. Dynamical processes in polar regions, incl. polar–midlatitude interactions. https://doi.org/10.5194/egusphere-2022-693

Dong, X., Wang, Y., Hou, S., Ding, M., Yin, B., & Zhang, Y. (2020). Robustness of the Recent Global Atmospheric Reanalyses for Antarctic Near-Surface Wind Speed Climatology. *Journal of Climate*, *33*(10), 4027–4043. https://doi.org/10.1175/JCLI-D-19-0648.1

Eyring, V., Bony, S., Meehl, G. A., Senior, C. A., Stevens, B., Stouffer, R. J., & Taylor, K. E. (2016). Overview of the Coupled Model Intercomparison Project Phase 6 (CMIP6) experimental design and organization. *Geoscientific Model Development*, *9*(5), 1937–1958. https://doi.org/10.5194/gmd-9-1937-2016

Farman, J. C., Gardiner, B. G., & Shanklin, J. D. (1985). Large losses of total ozone in Antarctica reveal seasonal ClOx/NOx interaction. *Nature 315*, 207–210. https://doi.org/10.1038/315207a0

https://doi.org/10.5194/egusphere-2025-3374
Preprint. Discussion started: 8 September 2025

Fogt, R. L., & Marshall, G. J. (2020). The Southern Annular Mode: Variability, trends, and climate impacts across the Southern Hemisphere. *WIREs Climate Change*, *11*(4), e652. https://doi.org/10.1002/wcc.652

Francis, D., Mattingly, K. S., Lhermitte, S., Temimi, M., & Heil, P. (2020). Atmospheric extremes triggered the biggest calving event in more than 50 years at the Amery Ice shelf in September 2019. *The Cryosphere 15(4),* 2147-2165. https://doi.org/10.5194/tc-2020-219

Friedlingstein, P., O'Sullivan, M., Jones, M. W., Andrew, R. M., Bakker, D. C. E., Hauck, J., Landschützer, P., Le Quéré, C., Luijkx, I. T., Peters, G. P., Peters, W., Pongratz, J., Schwingshackl, C., Sitch, S., Canadell, J. G., Ciais, P., Jackson, R. B., Alin, S. R., Anthoni, P., … Zheng, B. (2023). Global Carbon Budget 2023. *Earth System Science Data*, *15*(12), 5301–5369. https://doi.org/10.5194/essd-15-5301-2023

Gidden, M. J., Riahi, K., Smith, S. J., Fujimori, S., Luderer, G., Kriegler, E., Van Vuuren, D. P., Van Den Berg, M., Feng, L., Klein, D., Calvin, K., Doelman, J. C., Frank, S., Fricko, O., Harmsen, M., Hasegawa, T., Havlik, P., Hilaire, J., Hoesly, R., … Takahashi, K. (2019). Global emissions pathways under different socioeconomic scenarios for use in CMIP6: A dataset of harmonized emissions trajectories through the end of the century. *Geoscientific Model Development*, *12*(4), 1443–1475. https://doi.org/10.5194/gmd-12-1443-2019

Gillett, N. P., Shiogama, H., Funke, B., Hegerl, G., Knutti, R., Matthes, K., Santer, B. D., Stone, D., & Tebaldi, C. (2016). The Detection and Attribution Model Intercomparison Project (DAMIP v1.0)contribution to CMIP6. *Geoscientific Model Development*, *9*(10), 3685–3697. https://doi.org/10.5194/gmd-9-3685-2016

Goyal, R., Sen Gupta, A., Jucker, M., & England, M. H. (2021). Historical and Projected Changes in the Southern Hemisphere Surface Westerlies. *Geophysical Research Letters*, *48*(4), e2020GL090849. https://doi.org/10.1029/2020GL090849

Gu, Y., Katul, G. G., & Cassar, N. (2021). The Intensifying Role of High Wind Speeds on Air-Sea Carbon Dioxide Exchange. *Geophysical Research Letters*, *48*(5), e2020GL090713. https://doi.org/10.1029/2020GL090713

Gualtieri, G. (2022). Analysing the uncertainties of reanalysis data used for wind resource assessment: A critical review. *Renewable and Sustainable Energy Reviews*, *167*, 112741. https://doi.org/10.1016/j.rser.2022.112741

Hersbach, H., Bell, B., Berrisford, P., Hirahara, S., Horányi, A., Muñoz-Sabater, J., Nicolas, J., Peubey, C., Radu, R., Schepers, D., Simmons, A., Soci, C., Abdalla, S., Abellan, X., Balsamo, G., Bechtold, P., Biavati, G., Bidlot, J., Bonavita, M., … Thépaut, J. (2020). The ERA5 global reanalysis. *Quarterly Journal of the Royal Meteorological Society*, *146*(730), 1999–2049. https://doi.org/10.1002/qj.3803

https://doi.org/10.5194/egusphere-2025-3374
Preprint. Discussion started: 8 September 2025

Huguenin, M. F., Holmes, R. M., & England, M. H. (2022). Drivers and distribution of global ocean heat uptake over the last half century. *Nature Communications*, *13*(1), 4921. https://doi.org/10.1038/s41467-022-32540-5

Jarníková, T., Quéré, C. L., Rumbold, S., & Jones, C. (2025). Decreasing importance of carbon-climate feedbacks in the Southern Ocean in a warming climate. *Science Advances*.

Jena, B., Bajish, C. C., Turner, J., Ravichandran, M., Anilkumar, N., & Kshitija, S. (2022). Record low sea ice extent in the Weddell Sea, Antarctica in April/May 2019 driven by intense and explosive polar cyclones. *npj Climate and Atmospheric Science*, *5*(1), 19. https://doi.org/10.1038/s41612-022-00243-9

Jones, R. W., Renfrew, I. A., Orr, A., Webber, B. G. M., Holland, D. M., & Lazzara, M. A. (2016). Evaluation of four global reanalysis products using in situ observations in the Amundsen Sea Embayment, Antarctica. *Journal of Geophysical Research: Atmospheres*, *121*(11), 6240–6257. https://doi.org/10.1002/2015JD024680

Kalnay, E., Kanamitsu, M., Kistler, R., Collins, W., Deaven, D., Gandin, L., Iredell, M., Saha, S., White, G., Woollen, J., & others. (2018). The NCEP/NCAR 40-year reanalysis project. In *Renewable energy* (p. Vol1_146-Vol1_194). Routledge.

Keeble, J., Hassler, B., Banerjee, A., Checa-Garcia, R., Chiodo, G., Davis, S., Eyring, V., Griffiths, P. T., Morgenstern, O., Nowack, P., Zeng, G., Zhang, J., Bodeker, G., Burrows, S., Cameron-Smith, P., Cugnet, D., Danek, C., Deushi, M., Horowitz, L. W., … Wu, T. (2021). Evaluating stratospheric ozone and water vapour changes in CMIP6 models from 1850 to 2100. *Atmospheric Chemistry and Physics*, *21*(6), 5015–5061. https://doi.org/10.5194/acp-21-5015-2021

Kosaka, Y., Kobayashi, S., Harada, Y., Kobayashi, C., Naoe, H., Yoshimoto, K., Harada, M., Goto, N., Chiba, J., Miyaoka, K., Sekiguchi, R., Deushi, M., Kamahori, H., Nakaegawa, T., Tanaka, T. Y., Tokuhiro, T., Sato, Y., Matsushita, Y., & Onogi, K. (2024). The JRA-3Q Reanalysis. *Journal of the Meteorological Society of Japan. Ser. II*, *102*(1), 49–109. https://doi.org/10.2151/jmsj.2024-004

Kuhlbrodt, T., Jones, C. G., Sellar, A., Storkey, D., Blockley, E., Stringer, M., Hill, R., Graham, T., Ridley, J., Blaker, A., Calvert, D., Copsey, D., Ellis, R., Hewitt, H., Hyder, P., Ineson, S., Mulcahy, J., Siahaan, A., & Walton, J. (2018). The Low-Resolution Version of HadGEM3 GC3.1: Development and Evaluation for Global Climate. *Journal of Advances in Modeling Earth Systems*, *10*(11), 2865–2888. https://doi.org/10.1029/2018MS001370

Le Quéré, C., Rödenbeck, C., Buitenhuis, E. T., Conway, T. J., Langenfelds, R., Gomez, A., Labuschagne, C., Ramonet, M., Nakazawa, T., Metzl, N., Gillett, N., & Heimann, M. (2007). Saturation of the Southern Ocean CO 2 Sink Due to Recent Climate Change. *Science*, *316*(5832), 1735–1738. https://doi.org/10.1126/science.1136188

https://doi.org/10.5194/egusphere-2025-3374
Preprint. Discussion started: 8 September 2025

Li, M., Liu, J., Wang, Z., Wang, H., Zhang, Z., Zhang, L., & Yang, Q. (2013). Assessment of Sea Surface Wind from NWP Reanalyses and Satellites in the Southern Ocean. *Journal of Atmospheric and Oceanic Technology*, *30*(8), 1842–1853. https://doi.org/10.1175/JTECH-D-12-00240.1

Lucio-Eceiza, E. E., González-Rouco, J. F., García-Bustamante, E., Navarro, J., & Beltrami, H. (2019). Multidecadal to centennial surface wintertime wind variability over Northeastern North America via statistical downscaling. *Climate Dynamics*, *53*(1–2), 41–66. https://doi.org/10.1007/s00382-018-4569-5

Marshall, G. J. (2003). Trends in the Southern Annular Mode from Observations and Reanalyses. *Journal of Climate*, *16*(24), 4134–4143. https://doi.org/10.1175/1520-0442(2003)016<4134:TITSAM>2.0.CO;2

Marshall, J., & Speer, K. (2012). Closure of the meridional overturning circulation through Southern Ocean upwelling. *Nature Geoscience*, *5*(3), 171–180. https://doi.org/10.1038/ngeo1391

McLandress, C., Shepherd, T. G., Scinocca, J. F., Plummer, D. A., Sigmond, M., Jonsson, A. I., & Reader, M. C. (2011). Separating the Dynamical Effects of Climate Change and Ozone Depletion. Part II: Southern Hemisphere Troposphere. *Journal of Climate*, *24*(6), 1850–1868. https://doi.org/10.1175/2010JCLI3958.1

Molod, A., Takacs, L., Suarez, M., & Bacmeister, J. (2015). Development of the GEOS-5 atmospheric general circulation model: Evolution from MERRA to MERRA2. *Geoscientific Model Development*, *8*(5), 1339–1356. https://doi.org/10.5194/gmd-8-1339-2015

Morrison, A. K., Frölicher, T. L., & Sarmiento, J. L. (2015). Upwelling in the Southern Ocean. *Physics Today*, *68*(1), 27–32. https://doi.org/10.1063/PT.3.2654

Morrison, A. K., Hogg, A. M., & Ward, M. L. (2011). Sensitivity of the Southern Ocean overturning circulation to surface buoyancy forcing: SOUTHERN OCEAN OVERTURNING. *Geophysical Research Letters*, *38*(14). https://doi.org/10.1029/2011GL048031

Mulcahy, J. P., Jones, C., Sellar, A., Johnson, B., Boutle, I. A., Jones, A., Andrews, T., Rumbold, S. T., Mollard, J., Bellouin, N., Johnson, C. E., Williams, K. D., Grosvenor, D. P., & McCoy, D. T. (2018). Improved Aerosol Processes and Effective Radiative Forcing in HadGEM3 and UKESM1. *Journal of Advances in Modeling Earth Systems*, *10*(11), 2786–2805. https://doi.org/10.1029/2018MS001464

Polvani, L. M., Previdi, M., & Deser, C. (2011). Large cancellation, due to ozone recovery, of future Southern Hemisphere atmospheric circulation trends: OZONE RECOVERY AND SH CIRCULATION TRENDS. *Geophysical Research Letters*, *38*(4). https://doi.org/10.1029/2011GL046712

https://doi.org/10.5194/egusphere-2025-3374
Preprint. Discussion started: 8 September 2025

Previdi, M., & Polvani, L. M. (2014). Climate system response to stratospheric ozone depletion and recovery. *Quarterly Journal of the Royal Meteorological Society*, *140*(685), 2401–2419. https://doi.org/10.1002/qj.2330

Ramon, J., Lledó, L., Torralba, V., Soret, A., & Doblas-Reyes, F. J. (2019). What global reanalysis best represents near-surface winds? *Quarterly Journal of the Royal Meteorological Society*, *145*(724), 3236–3251. https://doi.org/10.1002/qj.3616

Schulzweida, U. (2023, October). CDO User Guide (Version 2.3.0). Zenodo. https://doi.org/10.5281/zenodo.10020800

Sellar, A. A., Jones, C. G., Mulcahy, J. P., Tang, Y., Yool, A., Wiltshire, A., O'Connor, F. M., Stringer, M., Hill, R., Palmieri, J., Woodward, S., Mora, L., Kuhlbrodt, T., Rumbold, S. T., Kelley, D. I., Ellis, R., Johnson, C. E., Walton, J., Abraham, N. L., … Zerroukat, M. (2019). UKESM1: Description and Evaluation of the U.K. Earth System Model. *Journal of Advances in Modeling Earth Systems*, *11*(12), 4513–4558. https://doi.org/10.1029/2019MS001739

Sellar, A. A., Walton, J., Jones, C. G., Wood, R., Abraham, N. L., Andrejczuk, M., Andrews, M. B., Andrews, T., Archibald, A. T., De Mora, L., Dyson, H., Elkington, M., Ellis, R., Florek, P., Good, P., Gohar, L., Haddad, S., Hardiman, S. C., Hogan, E., … Griffiths, P. T. (2020). Implementation of U.K. Earth System Models for CMIP6. *Journal of Advances in Modeling Earth Systems*, *12*(4), e2019MS001946. https://doi.org/10.1029/2019MS001946

Shi, J.-R., Talley, L. D., Xie, S.-P., Liu, W., & Gille, S. T. (2020). Effects of Buoyancy and Wind Forcing on Southern Ocean Climate Change. *Journal of Climate*, *33*(23), 10003–10020. https://doi.org/10.1175/JCLI-D-19-0877.1

Sohail, T., Gayen, B., & Klocker, A. (2025). Decline of Antarctic Circumpolar Current due to polar ocean freshening. *Environmental Research Letters*, *20*(3), 034046. https://doi.org/10.1088/1748-9326/adb31c

Solomon, S., Garciat, R. R., Rowland, F. S., & Wuebbles, D. J. (1986). On the depletion of Antarctic ozone.

Solomon, S., Ivy, D., Gupta, M., Bandoro, J., Santer, B., Fu, Q., Lin, P., Garcia, R. R., Kinnison, D., & Mills, M. (2017). Mirrored changes in Antarctic ozone and stratospheric temperature in the late 20th versus early 21st centuries. *Journal of Geophysical Research: Atmospheres*, *122*(16), 8940–8950. https://doi.org/10.1002/2017JD026719

Swart, N. C., & Fyfe, J. C. (2012). Observed and simulated changes in the Southern Hemisphere surface westerly wind-stress: CHANGES IN THE S.H. WESTERLIES. *Geophysical Research Letters*, *39*(16). https://doi.org/10.1029/2012GL052810

https://doi.org/10.5194/egusphere-2025-3374
Preprint. Discussion started: 8 September 2025

Thompson, D. W. J., & Solomon, S. (2002). Interpretation of Recent Southern Hemisphere Climate Change. *Science*, *296*(5569), 895–899. https://doi.org/10.1126/science.1069270

Thompson, D. W. J., Solomon, S., Kushner, P. J., England, M. H., Grise, K. M., & Karoly, D. J. (2011). Signatures of the Antarctic ozone hole in Southern Hemisphere surface climate change. *Nature Geoscience*, *4*(11), 741–749. https://doi.org/10.1038/ngeo1296

Tsujino, H., Urakawa, L. S., Griffies, S. M., Danabasoglu, G., Adcroft, A. J., Amaral, A. E., Arsouze, T., Bentsen, M., Bernardello, R., Böning, C. W., Bozec, A., Chassignet, E. P., Danilov, S., Dussin, R., Exarchou, E., Fogli, P. G., Fox-Kemper, B., Guo, C., Ilicak, M., … Yu, Z. (2020). Evaluation of global ocean–sea-ice model simulations based on the experimental protocols of the Ocean Model Intercomparison Project phase 2 (OMIP-2). *Geoscientific Model Development*, *13*(8), 3643–3708. https://doi.org/10.5194/gmd-13-3643-2020

Velasquez-Jimenez, L., & Abram, N. J. (2024). Technical note: An improved methodology for calculating the Southern Annular Mode index to aid consistency between climate studies. *Climate of the Past*, *20*(5), 1125–1139. https://doi.org/10.5194/cp-20-1125-2024

Wald, A. (1943). Tests of statistical hypotheses concerning several parameters when the number of observations is large. *Transactions of the American Mathematical Society*, *54*(3), 426–482.

Walters, D., Baran, A. J., Boutle, I., Brooks, M., Earnshaw, P., Edwards, J., Furtado, K., Hill, P., Lock, A., Manners, J., Morcrette, C., Mulcahy, J., Sanchez, C., Smith, C., Stratton, R., Tennant, W., Tomassini, L., Van Weverberg, K., Vosper, S., … Zerroukat, M. (2019). The Met Office Unified Model Global Atmosphere 7.0/7.1 and JULES Global Land 7.0 configurations. *Geoscientific Model Development*, *12*(5), 1909–1963. https://doi.org/10.5194/gmd-12-1909-2019

Waugh, D. W., Banerjee, A., Fyfe, J. C., & Polvani, L. M. (2020). Contrasting Recent Trends in Southern Hemisphere Westerlies Across Different Ocean Basins. *Geophysical Research Letters*, *47*(18), e2020GL088890. https://doi.org/10.1029/2020GL088890

Yool, A., Palmiéri, J., Jones, C. G., de Mora, L., Kuhlbrodt, T., Popova, E. E., Nurser, A. J. G., Hirschi, J., Blaker, A. T., Coward, A. C., Blockley, E. W., & Sellar, A. A. (2021). Evaluating the physical and biogeochemical state of the global ocean component of UKESM1 in CMIP6 historical simulations. *Geoscientific Model Development*, *14*(6), 3437–3472. https://doi.org/10.5194/gmd-14-3437-2021

Zambri, B., Solomon, S., Thompson, D. W. J., & Fu, Q. (2021). Emergence of Southern Hemisphere stratospheric circulation changes in response to ozone recovery. *Nature Geoscience*, *14*(9), 638–644. https://doi.org/10.1038/s41561-021-00803-3